

# **LES Study on Mechanism of Reduction of Shock Induced Flow Separation by MVG**

**Yong Yang  
Yonghua Yan  
Chaoqun Liu**

**Technical Report 2014-14**

# LES Study on Mechanism of Reduction of Shock Induced Flow Separation by MVG

Yong Yang, Yonghua Yan, Chaoqun Liu

*University of Texas at Arlington, Arlington, Texas, 76019, USA*

## Abstract

Shock-boundary layer interaction (SBLI) is a kind of problem which is frequently met in supersonic engine inlet flow and external flow. A detail study on mechanism of reduction of shock induced flow separation by MVG is carried out by high order implicit large eddy simulation (LES). To generate the fully developed turbulent flow, a series of turbulent profiles are given by previous DNS simulation results. The mechanism of reduction of shock induced flow separation was originally considered as a result of plump velocity profile caused by turbulent kinetic energy. It was acclaimed that turbulent flow has so stronger kinetic energy that the velocity profile is changed to be plump, which lead to reduction of shock induced flow separation. However, according to our detail study in this paper, the shock wave breaks down when ring-like vortices generated by MVG are passing through it, while the vortex structure never breaks down and is even little influenced. Therefore, the flow separation induced by shock is reduced by break-down of shock wave, not plump velocity profile. More details of the investigation on the mechanism are reported in this paper.

**Keywords:** SBLI, MVG, LES, shock, separation

## Nomenclature

MVG = micro ramp vortex generator  
 $M$  = Mach number  
 $Re_\theta$  = Reynolds number based on momentum thickness  
 $h$  = micro ramp height  
 $\delta$  = incompressible boundary-layer nominal thickness  
 $x, y, z$  = spanwise, normal and streamwise coordinate axes  
 $u, v, w$  = spanwise, normal and streamwise velocity

### Subscript

$0$  = inlet  
 $w$  = wall  
 $\infty$  = free stream

## I. Introduction

Micro vortex generators (MVG) are a kind of low-profile passive control device designed for the boundary layer control, which was considered to be very practical for the flow control in supersonic. In contrast to the conventional counterpart, MVG has the smaller size (approximately the height 20-40% of the boundary layer), longer streamwise distance for the vortices to remain in the boundary layer, and therefore better efficiency of the

momentum exchange [1] [2]. In Lin's review [3] on the low-profile vortex generator, it was mentioned that MVG could alleviate the flow distortion in compact ducts to some extent and control boundary layer separation due to the adverse pressure gradients. Similar comments were made in the review by Ashill et al [4].

Supersonic ramp flow is a typical prototype SBLI problem, and the ramp configuration often exists on the engine and control surfaces in high speed vehicles. The fundamental problem of the ramp flow includes the determination of characteristics and criteria of the flow separation and reattachment, the mechanism of the shock unsteadiness, and the aerodynamic/thermal correspondence, etc. For experimental investigations, some well recognized studies can be found from the work by Dolling [5], Settles [6], Dussauge [7], Andreopoulos [8], Loginov [9]. And many numerical simulations had been made on these problems as well, such as simulations on a compression corner by implicit LES using a high-order method made by Rizzetta and Visbal [10]; LES on ramp flow conducted by Kaenal, Kleiser and Adams et al [11] which used an approximate de-convolution model developed by Stolz Martin [12] [13]. More work on MVG and other flow control tools have been done recently. According to the experimental and numerical research, some flow mechanisms are recognized as: a) the amplification of the turbulence after the SBLI is thought to be caused by the nonlinear interaction between the shock wave and the coupling of turbulence, vorticity and entropy waves [14]; b) the unsteady motion of the shock is considered to be generated by the very long low-momentum coherent structures in logarithmic layer and such structures might be formed by the hairpin vortex packet.

The mechanism of how the MVG can be used to control the supersonic ramp flow is still need to study, although there are many investigation of experiments and computations on MVG and ramp problems. A new model of five pairs of the vortex tubes around MVG (Fig.1) was given by Li and Liu [15] [16], after analyses on numerical simulations about MVG controlled flow using LES at  $M=2.5$  and  $Re=1440$ . The dominant vortex near the MVG is the primary vortex; underneath there are two first secondary counter-rotating vortices, which later leave the body surface and become fully 3D separations by the way of spiral points in body surface. These vortices will merge into the primary vortex propagating downstream, while new secondary vortex will be generated under the primary vortex. This dynamic vortex model is mostly confirmed by the experiment work of Mohd R. Saad et al [17] (Fig. 2).

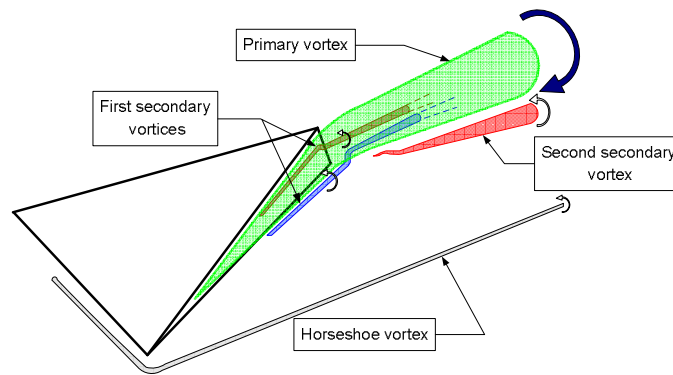


**Figure 1: The dynamic vortex model (Li and Liu)**

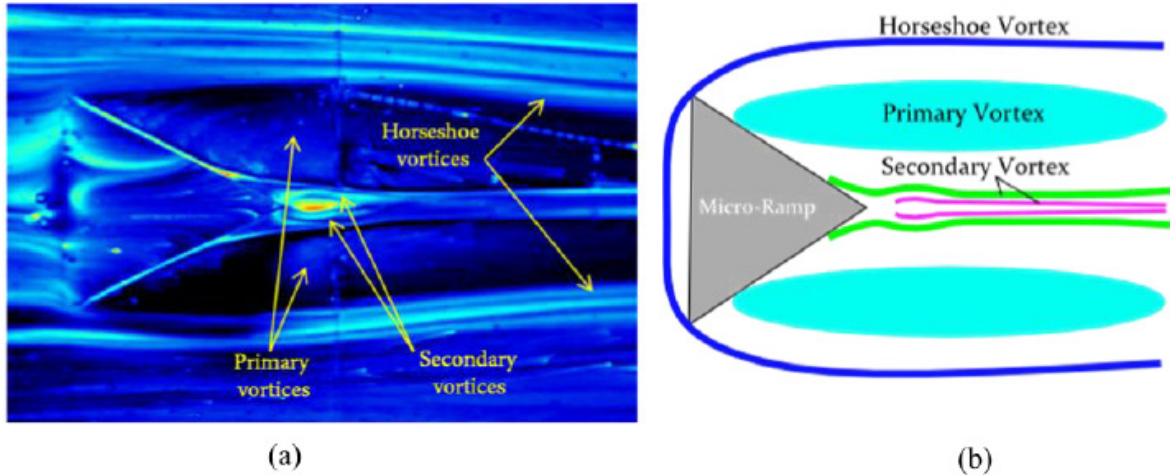


**Figure 2. Surface flow visualisation image and the vortex model given by Mohd R. Saad<sup>26</sup> et al**

In our previous studies [18] [19], numerical simulations are made on supersonic ramp flow with MVG control at  $M=2.5$  and  $Re=5760$ . The flow field around the MVG and surrounding areas has been studied in details. Furthermore, 3-D structure of the shocks is also obtained. The special ring-like vortices were found and they would travel to downstream. After the MVG, a strong momentum deficit was found behind MVG which causes a strong circular shear layer [20], which is consistent with the referenced computations and experiments. To reveal the coherent structure of the flow, the iso-surface of  $\lambda_2$  scalar field is given in Fig. 3. It is very clear that there is a chain of vortex rings, starting from behind of the trailing-edge of MVG. Compared to the vortex structure in MVG controlled low intensity turbulent boundary layer [21], the ring-like vortex structure is still generated if the inlet condition is fully developed turbulent inflow. These rings could be a dominant factor of the mechanisms of MVG in control of shock boundary layer interaction.

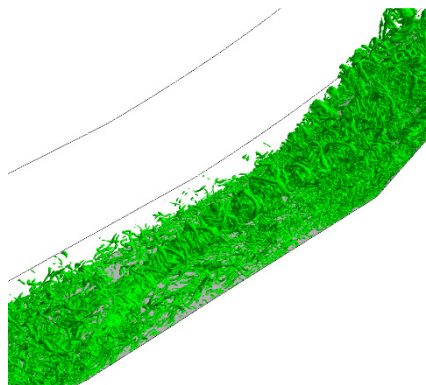
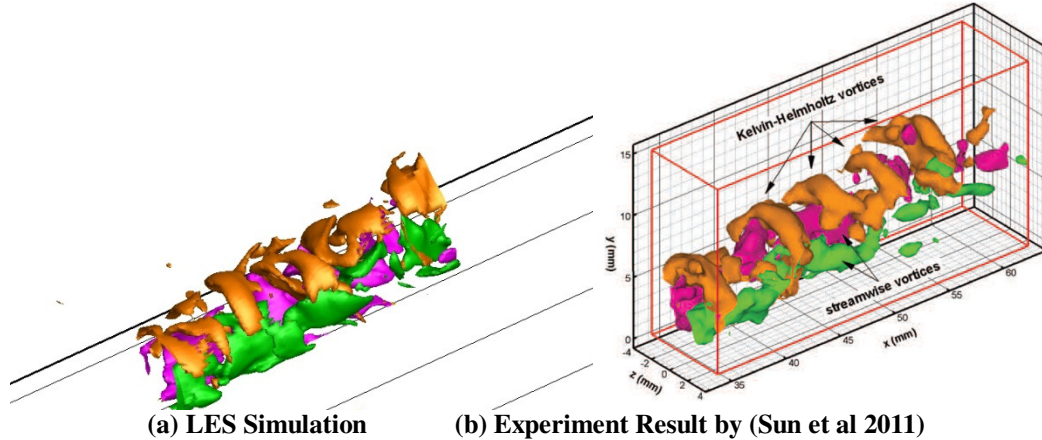


**Figure 3. Vortex rings shown by iso-surface of  $\lambda_2$**

Numerical discoveries of the vortex ring structures in our previous papers is also confirmed by 3-D PIV experiment (Fig. 4b) conducted by Sun et al [22] at Delft University. The particle image velocimetry (PIV) and the acetone vapor screen visualization are used to track the movement of the flow. Compared the two results(Fig. 4), we can find the similar distribution of streamwise and spanwise vorticity components, which also proves the existence of ring structures.



(a) LES Simulation (b) Experiment Result by (Sun et al 2011)  
**Figure 4. Distribution of Kelvin-Helmholtz vortices and streamwise vortices**

In this paper, the interaction between shock wave and ring-like vortices generated by MVG is studied in detail, and the mechanism of reduction of shock induced flow separation by MVG is further studied.

## II. Numerical methods, grid generation and turbulent inflow

To reveal the mechanism and get deep understanding of MVG, high order DNS/LES is necessary. In this paper, a method called monotone integrated LES (MILES) [10] was used for solving the unfiltered form of the Navier-Stokes equations with the 5th order bandwidth-optimized WENO scheme at  $\beta = 70^\circ$ , in which the numerical dissipation is used as the sub-grid stress model.

Flows around MVGs are studied with back edge declining angle  $70^\circ$  (see Fig. 8a). The geometries for the cases are shown in Fig 8b. (in which  $\delta_0$  represents the incompressible boundary layer nominal thickness). The grid number for the whole system is:  $n_{\text{spanwise}} \times n_{\text{normal}} \times n_{\text{streamwise}} = 128 \times 192 \times 1600$ .

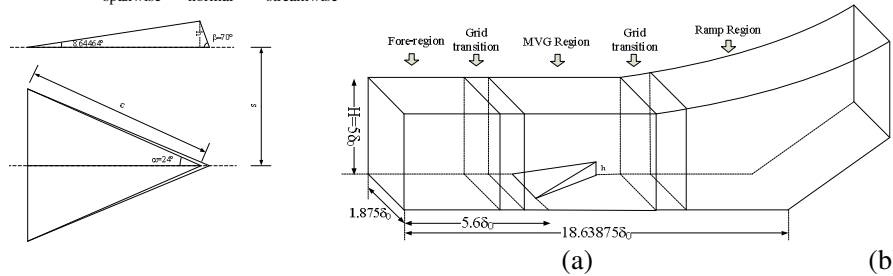


**Figure 8. (a) The sketch of MVG at  $\beta=70^\circ$  (b) The schematic of the half grid system**

The details about the geometric objects, grid generation, computational domain, etc, which are introduced in our previous paper [18] [20] [21], will not be repeated here.

The adiabatic, zero-gradient of pressure and non-slipping conditions are adopted at the wall. To avoid possible wave reflection, the non-reflecting boundary conditions are used on the upper boundary. The boundary conditions at the front and back boundary surfaces in the spanwise direction are treated as the periodic condition, which is under the consideration that the problem is about the flow around MVG arrays and only one MVG is simulated. The outflow boundary conditions are specified as a kind of characteristic-based condition, which can handle the outgoing flow without reflection.

To generate the true turbulent inlet, twenty thousand turbulent profiles are obtained from previous DNS simulation and used as the time dependent inflow [23]. In our previous paper, the flow properties were also checked. It provides a shape factor  $H$  as about 1.35, which shows the flow before the MVG is fully developed turbulence flow. The inflow boundary layer velocity profile agrees with the analytical profile as well.

To check the flow properties before the MVG, we analyzed the relevant flow parameters on a spanwise cross section which is  $11.97h$  ahead the apex of MVG. As a result, the displacement thickness  $\delta^* = 0.371h$ , the momentum thickness  $\theta = 0.275h$ , nominal boundary layer thickness  $\delta = 2.36h$ . Thus, we can obtain a shape factor  $H$  as about 1.35, which shows the flow before the MVG is fully developed turbulence flow.

Fig. 9 shows the inflow boundary layer velocity profile in log-coordinates on the same cross section. There is a well-defined log region and the agreement with the analytical profile is well established. These results are typical for a naturally grown turbulent boundary layer in equilibrium.

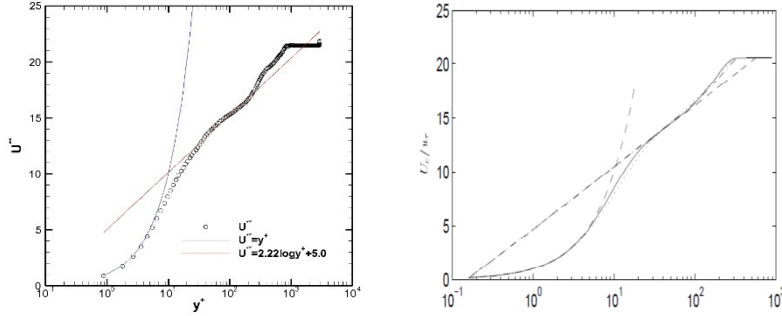


**Figure 9. Inflow boundary-layer profile comparison with Guarini et al's<sup>31</sup>**

### III. Analyses on reduction of shock induced flow separation by MVG (Still working on it)

#### 1. The ring-like vortices never broke down

The newly generated vortex ring will immediately interact with the shock wave induced by the ramp. The ring-like vortex would pass through the shock wave rather smoothly and kept its topology structure and even its velocity after passing. In Fig. 5, the streamwise vorticity distributions on the central plane before and after a ring-like vortex passing through the shock wave are given. The typical high value centers present the positions of the vortex tops on the central plane. It shows that the ring-like vortex does not break down at the top part and even the vorticity distribution in it does not influenced much by the shock wave. Fig. 6 shows the 3D vortex lines starting from a ring-like vortex top which just passed through the shock. Vortex ring structure is composed by the vortex lines. From Fig 6, we can see the concentration of the vortex lines at the top of the vortex which forms the ring structure, and those lines scatter to the space in the bottom. As a strong shock wave, it generates the strong discontinuity to velocity, density and pressure. However, the vortex lines which compose the ring structure is not broken at the region of the shock, they connect the two flow field separated by the shock. This is another proof to show that the ring structure is quite robust, never break down during the interaction and even be little influenced by the existence of shock wave.

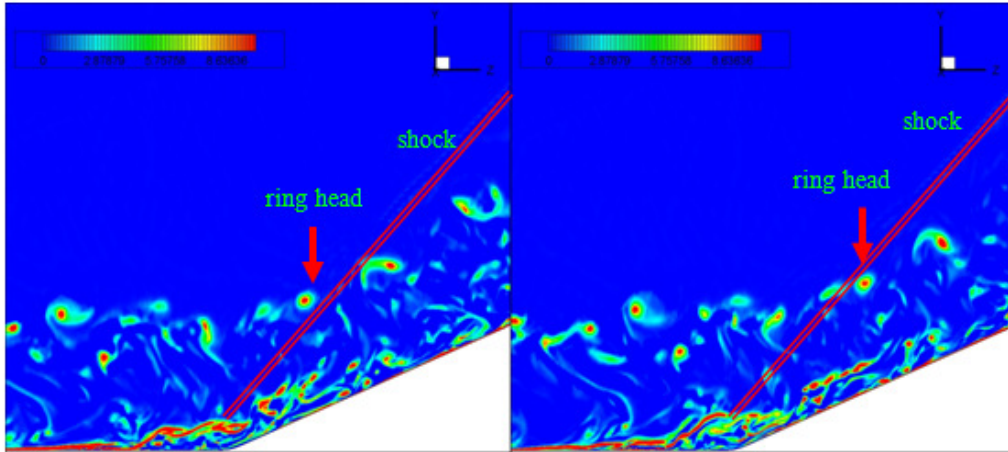


**Figure 5. Streamwise vorticity distribution at two sequential different time steps**

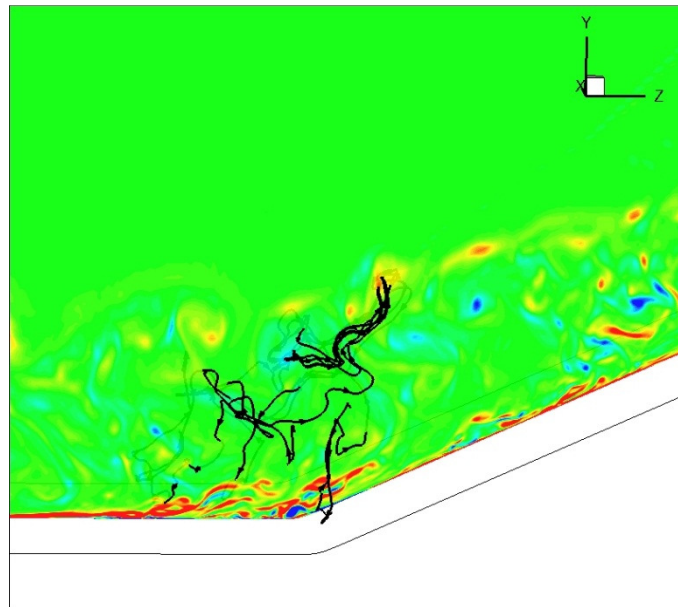


**Figure 6. Vortex lines pass through a ring head after the shock**

## 2. The shock wave breaks down

When the vortex rings generated by MVG are passing through shock wave induced by ramp, shock wave would break down. During the interaction, the shock wave at the ramp corner was distorted badly and even was reduced a lot. In Fig. 7, we can see that the quantity of the shock wave is reduced a lot at the region where the interaction happens. It shows the upper part of the shock wave keeps well in the shape. In the meanwhile, at the bottom part, it suffers the severe interaction. Fig. 7 also shows the pressure and density gradient distribution before and after a ring-like vortex passing through the shock wave. During the process, a structure of multiple layer shock waves is discovered. This typical multiple layer shock structure is continuously formed when ring-like vortices pass through the shock wave. The number of the shock layers changes during the interaction, generally, 2-4 layers will be formed. As we mentioned in previous paper, by the upward induction of the flow at the center position of the ring, a particular bump shape will be formed after a ring's penetration. Here, the mechanism of the multiple layer shock wave can also be explained by the influence of the rings. Actually, the bump shape is the most outer side layer of the shocks. When a vortex ring penetrates the shock, the upward induction on the flow will generate a new shock layer which is much weaker than the shock at the upper part. However, the new born weak shock layer does not

disappear immediately after the ring passed the shock. When the second ring afterwards comes, another shock layer will be formed. This is the mechanism of the multiple layer shock waves and the relation to the arc-like bump shape. However, the multiple layer structure will disappear after the interaction with a certain ring-like vortex.

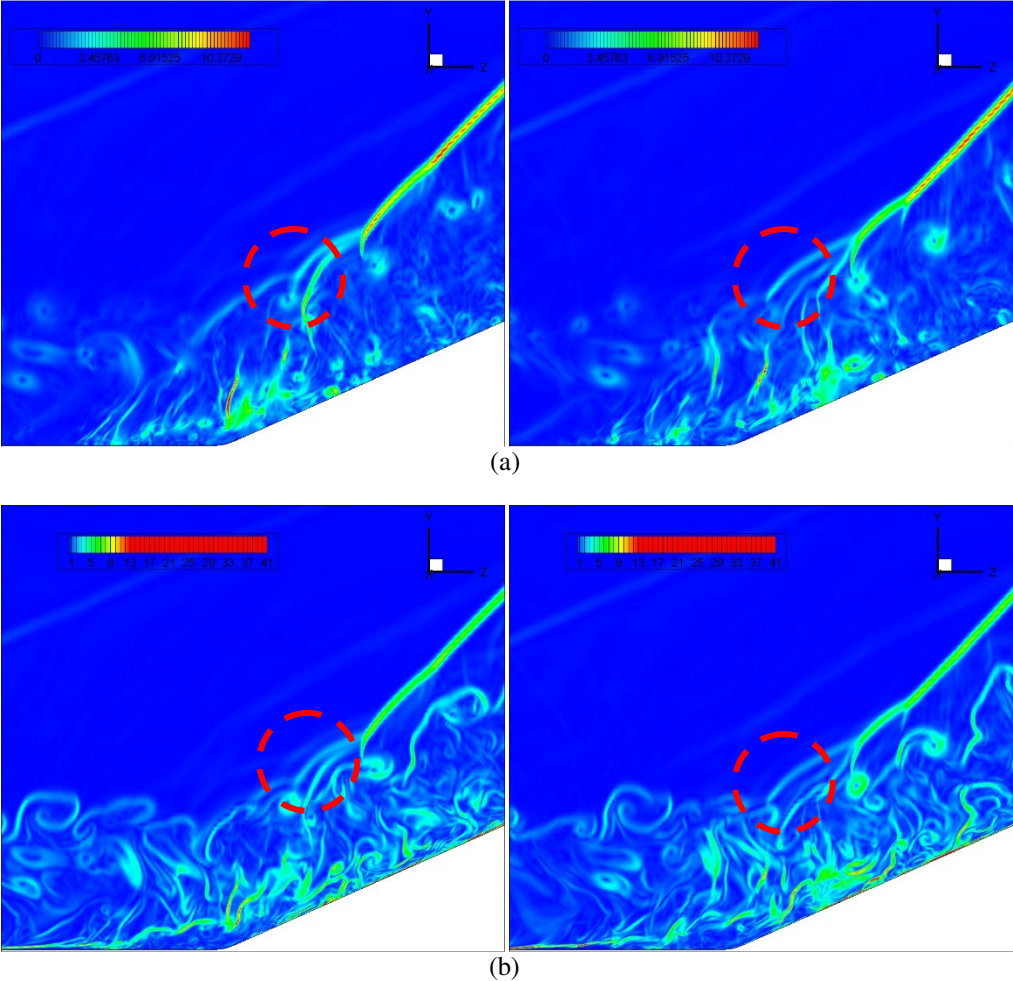


**Figure 7. Pressure gradient (a) and density gradient (b) at two sequential time steps**

The flow field lost its symmetry and it can be clearly illustrated by the shape of shock wave. The shock wave shape is in fully 3D when shock wave and vortex rings are interacting (Fig. 8). When a ring-like vortex passes through the shock wave, a bump of the 3D shock wave surface is present. It showed that when a ring-like vortex enters the shock wave, it would incline to some degree to the ramp which will cause upward induction of the flow at the center position of the ring. The inducted flow will interact with the incoming free stream and make the surface of the shock wave to be an obvious arc-like boundary.

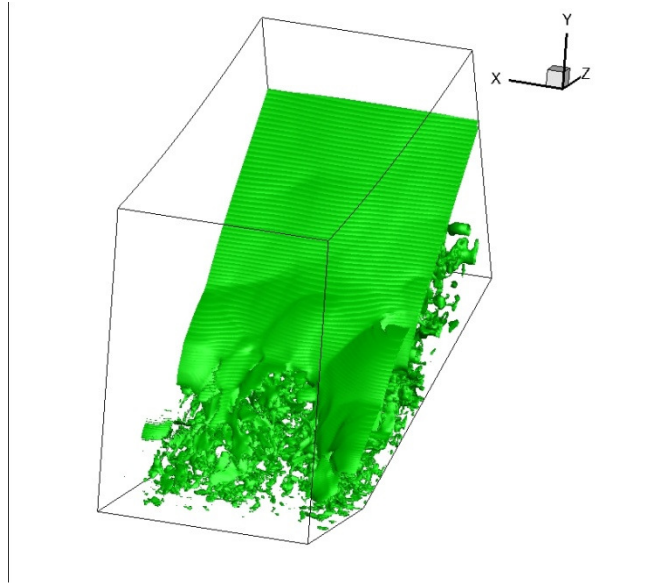


**Figure 8. Time averaged iso-surface of pressure gradient**

### **3. mechanism of reduction of shock induced flow separation by MVG**

The pressure at the center of vortex rings is lower than surroundings. When vortex rings are passing through the shock wave, they will change the pressure distribution around shock wave. In fact, the pressure before shock wave will decrease due to vortex rings, and then the difference of pressure between front and back of shock wave will reduce. Therefore, the shock wave is distorted badly and even is reduced a lot since the shock is a result of difference of pressure. **More quantity researches will be reported in the final AIAA paper.**

### **IV. Conclusion**

The mechanism of reduction of shock induced flow separation was originally considered as a result of plump velocity profile caused by turbulent kinetic energy. It was acclaimed that turbulent flow has so stronger kinetic energy that the velocity profile is changed to be plump, which lead to reduction of shock induced flow separation. However, according to this detail study, the shock wave breaks down when vortices are passing through it, while the vortex structure never breaks down and is even not influenced. The lower pressures at the center of vortex rings reduce the difference of pressure between front and back of shock wave, and then change the shock wave profile and structure. Therefore, the flow separation induced by shock is reduced by break-down of shock wave, not plump velocity profile.

### **References**

- [1] Babinsky, H., Li, Y., Ford, C. W. P., "Microramp Control of Supersonic Oblique Shock-Wave/Boundary-Layer Interactions," *AIAA J.*, vol. 47, no. 3, pp. 668-675, 2009.
- [2] Ghosh, S., Choi, J., and Edwards, J. R., "Numerical Simulations of the Effects of Micro Vortex Generators Using Immersed Boundary Methods," *AIAA J.*, vol. 48, no. 1, 2010.
- [3] L. J. C., "Review of Research on Low-Profile Vortex Generators to Control Boundary-Layer Separation," *Progress in Aerospace Sciences*, vol. 38, pp. 389-420, 2002.
- [4] Ashill, P. R., Fulker, J. L., Hackett, K. C., "A Review of Recent Developments in Flow Control." , 109, 1095, pp.205-232(2005).," *The Aeronautical Journal*, vol. 109, no. 1095, pp. 205-232, 2005.

- [5] D. S. Dolling, "Fifty Years of Shock-Wave/Boundary-Layer Interaction Research: What next?," *AIAA J.*, vol. 39, pp. 1517-1531, 2001.
- [6] Settles, G. S., Dodson, L. J., "Supersonic and Hypersonic Shock/Boundary Layer Interaction Database," *AIAA J.*, vol. 32, no. 1994, pp. 1377-1383.
- [7] Dussauge, J. P., Dupont, P., Debieve, J. F., "Unsteadiness in Shock Wave Boundary Layer Interaction with Separation," *Aerospace Science and Technology*, vol. 10, no. 2, pp. 85-91, 2006.
- [8] Andreopoulos, J., Agui, J. H., Briassulis, G., "Shock Wave-Turbulence Interactions," *Annu. Rev. Fluid Mech.*, vol. 32, pp. 309-345, 2000.
- [9] Loginov, M. S., Adams, N. A., Zheltovodov, A. A., "Large-Eddy Eimulation of Shock-Wave/Turbulent-Boundary-Layer Interaction," *J. Fluid Mech.*, vol. 565, pp. 135-169, 2006.
- [10] Rizzetta, D., Visbal, M., "Large Eddy Simulation of Supersonic Compression-Ramp Flow by High-Order Method," *AIAA J.*, vol. 39, no. 12, pp. 2283-2292, 2001.
- [11] Kaenel, R.V, Kleiser, L. Adams, N. A. Vos, J. B., "Large-Eddy Simulation of Shock-Turbulence Interaction," *AIAA J.*, vol. 42, no. 12, pp. 2516-2528, 2004.
- [12] Ringuette, M. Wu, M., Martín, M. P., "Low Reynolds Number Effects in a Mach 3 Shock/Turbulent-Boundary-Layer Interaction," *AIAA J.*, vol. 46, no. 7, pp. 1884-1887, 2008.
- [13] M. M. M. P. Wu, "Analysis of Shock Motion in Shockwave and Turbulent Boundary Layer Interaction Using Direct Numerical Simulation Data," *J. Fluid Mech.*, vol. 594, p. 71-83, 2008.
- [14] Marxen, O., Rist, U., "Mean Flow Deformation in a Laminar Separation Bubble: Separation and Stability Characteristics," *Journal of Fluid Mechanics*, vol. 660, pp. 37-54, 2010.
- [15] Q. Li, C. Liu, "LES for Supersonic Ramp Control Flow Using MVG at  $M=2.5$  and  $Re=1440$ ," AIAA, 2010.
- [16] Q. Li, C. Liu, "Numerical Investigations on the Effects of the Declining angle of the trailing-edge of MVG," *AIAA Journal of Aircraft*, vol. 47, no. 6, pp. 2086-2095, 2011.
- [17] Mohd R. Saad, Hossein Zare-Behtash, Azam Che Idris and Konstantinos Kontis, "Micro-Ramps for Hypersonic Flow Control," *Micromachines*, 2012, 3, 1-x manuscripts; doi:10.3390/mi30x000x.
- [18] Yonghua Yan, Caixia Chen, Ping Lu, Chaoqun Liu, "Study on Shock wave-Vortex Ring Interaction by the MVG Controlled Ramp Flow with turbulence inlet from DNS," AIAA, 2012.
- [19] Yonghua Yan, Chaoqun Liu, "Further Investigation on the Physics of Shock Wave -Vortex Interaction In MVG Controlled Ramp Flow," AIAA, 2013.
- [20] Yonghua Yan, Qin li, Chaoqun Liu, Adam Pierce, and Frank Lu., "Numerical Discovery and Experimental Confirmation of Vortex Ring Generation by Microramp Vortex Generator," *Applied Mathematical Modelling*, vol. 36, p. 5700-5708, 2012.
- [21] Qin Li, Yonghua Yan, Chaoqun Liu, "Numerical and Experimental Studies on the Separation Topology of the MVG Controlled Flow," AIAA, 2011-72.
- [22] Sun, Z., Schrijer, F.F.J., Scarano, F., and Oudheusden, B.W.V., "PIV Investigation of the 3D Instantaneous Flow Organization behind a Micro-Ramp in a Supersonic Boundary Layer," University of Delft, ISSW28,

Manchester, UK, July 17-22, 2011.

- [23] Liu, C. and Chen, L., "Study of Mechanism of Ring-Like Vortex Formation in Late Flow Transition," AIAA, 2010-1456.